Geomorphology 354 (2020) 107033

Contents lists available at ScienceDirect

Geomorphology

journal homepage: www.elsevier.com/locate/geomorph

Glacial and fluvial erosion in the Dolpo Basin, Western Nepal

Rhys E. Buceta [a,*], Lindsay M. Schoenbohm [a,b], Peter G. DeCelles [c]

[a] Department of Chemical and Physical Sciences, University of Toronto Mississauga, Mississauga, Ontario L5L 1C6, Canada
[b] Department of Earth Sciences, University of Toronto, Toronto, Ontario M5S 3B1, Canada
[c] Department of Geosciences, University of Arizona, Tucson, AZ 85716, USA

ARTICLE INFO

Article history:
Received 13 June 2019
Received in revised form 1 January 2020
Accepted 8 January 2020
Available online 10 January 2020

Keywords:
Glacial morphology
Glacial erosion
River capture
Himalayas
Tibet
Landscape evolution

ABSTRACT

The landscape of Western Nepal has been dramatically shaped by tectonics and by both glacial and fluvial erosion. Here we investigate the modern geomorphic and glacial features of the Dolpo basin in northern mid-western Nepal. We analyze attributes such as glacier size, slope, aspect and toe, head and peak elevation for 446 glaciers within and around the basin, determining their relationship with basin features such as lithology, slope and precipitation. Glaciers reflect lithology and precipitation, but glacier size is strongly correlated with base-level and slope. Our data suggest that low-slope glaciers with high base-level, i.e., those that flow onto the Tibetan plateau, are forced to grow large because they exist at or above the equilibrium-line altitude. Glaciers within the basin, particularly in the western part, can become dismembered on steep slopes, an effect only partly offset by precipitation. The spatial variability in regional slope and presence of a wind gap along the northern basin border suggest recent capture of the Dolpo basin. A plateau-like morphology would have thus once extended at least 45 km southward. The southward opening of the basin allowed precipitation to enter, forming glaciers along the western end of the northern basin border. Larger glaciers (resulting from high base-level) pushed the ridge southward over time through headward erosion. Our study suggests dramatic landscape reorganization in western Nepal, consistent with other recent studies suggesting a more extensive proto-Tibet.

1. Introduction

Recent work suggests the Tibetan plateau may once have extended south of its present position. For example, low-temperature thermochronology [Carrapa et al., 2016] shows profound asymmetry in ages across the modern Himalayan drainage divide, arguing for significant erosional exhumation and progressive northward divide migration. Other recent studies have identified low-relief, high-elevation surfaces south of the drainage divide that could be remnants of a more extensive proto-Tibetan plateau, although the authors of these studies have attributed them to other causes, including recent uplift above a mid-crustal ramp in western Nepal [Harvey et al., 2015], and the fluvial response to duplexing in Bhutan [Adams et al., 2016].

If the Tibetan plateau has retreated to the north since the Pliocene, it is important to constrain whether and how that could have been accomplished. Fluvial erosion can cause divide migration [e.g.,Willett et al., 2014] and dramatic reorganization of even continent-scale drainage networks [e.g., Clark et al., 2004]. Glaciers can also cause major reorganization of a landscape [e.g., Shugar et al., 2017], and are known to cause divide migration [Brocklehurst et al., 2002; Dortch et al., 2011; Schoenbohm et al., 2014]. Additionally, glaciers are sensitive to lithology [Ward et al., 2012] as well as evolving climate and local topography [Pedersen and Egholm, 2013; Pedersen et al., 2014].

In order to explore the landscape evolution of Tibet and the Himalaya, we focused on the Dolpo drainage basin in Western Nepal. Despite high shortening rates [Robinson et al., 2006; Bhattacharyya and Ahmed, 2016], the elevation is relatively low [e.g. Hannah et al., 2005]. Additionally, there is evidence for recent, dramatic uplift or base-level change within the landscape based on study of the fluvial system [Cannon and Murphy, 2014]. Hundreds of glaciers are present within and around the basin; they vary significantly in size and are distributed irregularly. Sinuosity of the drainage divide correlated with the presence or absence of glaciers suggests glacial erosion may play a role in driving divide migration. These preliminary observations suggest the Dolpo basin has experienced recent changes that could reflect evolution of the position of the southern margin of the Tibetan plateau.

This study aims to unify our understanding of the glacial and fluvial landscape evolution of mid-western Nepal. To accomplish this, we mapped and cataloged 446 glaciers in and around the Dolpo basin, documenting characteristics such as area, slope, glacier length, and peak elevation. We examine controls on glaciation, including precipitation, lithology and base-level. We also identified important features in the topography, including differences in slope within the basin and the presence of at least two wind gaps. Taken together, our data indicate

* Corresponding author.
E-mail address: rhys.buceta@mail.utoronto.ca (R.E. Buceta).

https://doi.org/10.1016/j.geomorph.2020.107033

that while glaciers have the potential to cause divide migration, in the case of the Dolpo basin, the effect of glaciers has been to cause minor southward movement of the divide through headwall erosion by large glaciers developed on the Tibetan plateau, controlled by a high base-level. However, we also observe evidence for a major (40 km) northward migration of the divide that resulted from river capture. Our study points to important new controls on glacier form and erosive ability. We also provide support for the idea that a proto-Tibet could have extended farther south, with subsequent northward migration and gradual dissection of the landscape as a result of river capture.

2. Background

2.1. Basin characteristics

The Dolpo basin is a remote, westward-draining basin located in western Nepal within the Tibetan Himalayan zone, directly south of the Nepal-China border. The Dolpo basin is part of geologic Tibet [e.g., Fuchs, 1973; Fuchs, 1977]; however, the Dolpo basin is not part of geomorphic Tibet (also referred to as the Tibetan plateau). The Tibetan plateau is a region north of the Himalayas characterised by internal drainage and low-relief. The Dolpo basin is not internally drained, but rather is drained by rivers that ultimately flow southward across the frontal Himalayan thrust belt. It is also heavily incised, more physiographically similar to the Himalayas. The basin is elongated east-west (45 km × 100 km), with a base-level of ~2300 m. The tallest peak along the Dolpo basin's drainage divide, Kanjiroba, at an elevation of 6883 m, sits on the basin's southern border. The Dolpo basin is drained by the Mugu Karnali, which joins the larger Karnali River basin which drains most of the western third of Nepal, dropping to a base-level of ~200 m, prior to the river's exit from the mountains. North of the Dolpo basin, the Yarlung River drains much of southern Tibetan plateau with a base-level of ~3500 m, prior to the river's exit from the Tibetan plateau near the Namche Barwa syntaxis.

More than 400 glaciers lie around and within the Dolpo basin. Rock glaciers are common as well [Jones et al., 2018]. Only glaciers north of the basin's northern border have been mapped for flow velocity [Scherler et al., 2011], which was found to be relatively slow (<60 m/yr). Based on a regional study that included Dolpo basin glaciers, glacier mass balance is −0.32 m/yr [Kääb et al., 2012]. Glaciers in this region cluster around the margins of the Dolpo basin (Fig. 1). The largest and most abundant glaciers are located along the northern and southern divides, with smaller, sparser glaciers to the far west and east. Temperature and precipitation effects on glaciers are well described by the equilibrium-line altitude (ELA) [e.g. Ohmura et al., 1992]. Although, literature relating to ELA estimates and measurements in western Nepal is scarce, ELA values in central and eastern Nepal have been reported to range between 5000 and 5800 m [Duncan et al., 1998; Kayastha and Harrison, 2008; Wagnon et al., 2013].

2.2. Basin geology

The Dolpo basin straddles a number of stratigraphic and structural units of the High Himalaya (Fig. 2). Neoproterozoic-Cambrian Greater Himalayan Sequence (GHS) rocks are juxtaposed with structurally underlying Paleoproterozoic Lesser Himalayan Sequence (LHS) rocks along the Main Central thrust (MCT). The GHS consists of amphibolite facies metasedimentary and igneous rocks, along with widespread early Miocene leucogranite bodies [Carosi et al., 2010; Iaccarino et al., 2017; Montomoli et al., 2013]. The northern part of the Dolpo basin contains a large body of Oligo-Miocene leucogranite, and other smaller outcrops are present to the west of Dolpo basin [Bertoldi et al., 2011]. The Dolpo basin is dominated by Ordovician-Jurassic rocks of the Tethyan Sedimentary Sequence (TSS). The TSS is separated from the GHS by the South Tibetan detachment system (STDS), a group of top-to-the-north low-angle normal faults which form a local syncline in the Dolpo region [e.g., Burg et al., 1984; Burchfiel et al., 1992; Fuchs and Poudel, 1998; see review by Kellett et al., 2018]. The TSS is composed of two separate sub-units: Ordovician (or possibly upper Cambrian) to upper Carboniferous phyllites and quartzites, and stratigraphically higher, Mesozoic un-metamorphosed sandstone and limestone. This upper unit crops out prominently in the eastern portion of the basin and north of the basin's northern drainage divide. TSS rocks are folded along NW-SE trending axes [Fuchs, 1973; Cannon and Murphy, 2014].

3. Methodology

3.1. Datasets

Glaciers were mapped on Landsat 7 1999–2003 Landsat ETM+ imagery accessed through the United States Geological Survey's EarthExplorer database (https://earthexplorer.usgs.gov/); newer

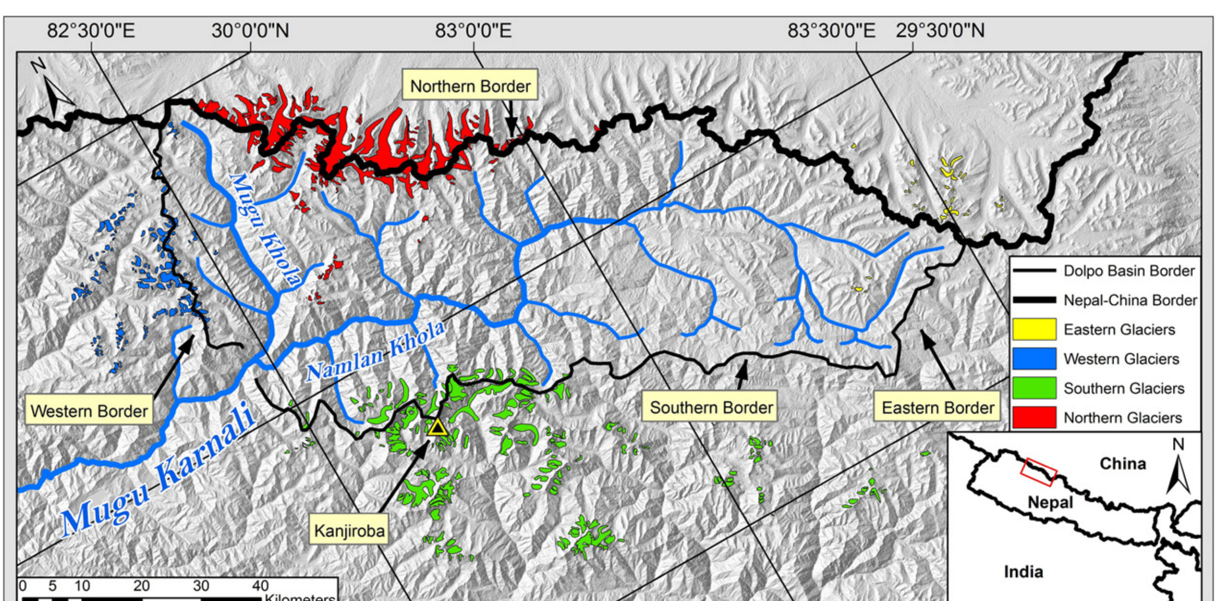

Fig. 1. Base map of the Dolpo basin highlighting the outlines of 446 glaciers mapped in this study.

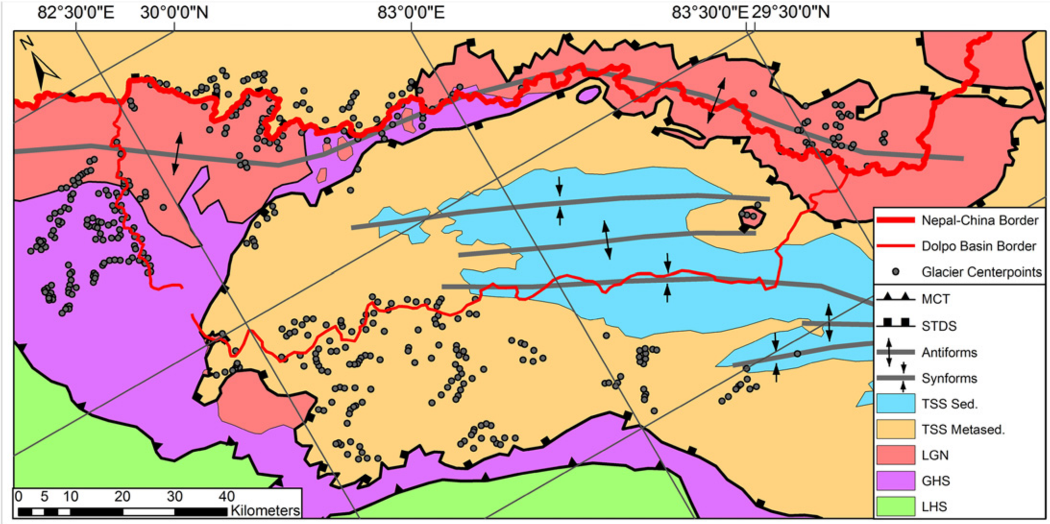

Fig. 2. Geologic map of the Dolpo basin compiled from Fuchs, 1964, 1967, 1973, 1977; Fuchs and Frank, 1970; Frank and Fuchs, 1970; Bertoldi et al., 2011; Cannon and Murphy, 2014. MCT = Main Central Thrust, STDS = South Tibetan Detachment System, TSS = Tethyan Sedimentary Sequence, LGN = Miocene leucogranite, GHS = Greater Himalayan Sequence, LHS = Lesser Himalayan Sequence, Sed = Sedimentary Rocks, Metased = Metasedimentary Rocks.

images are affected by the Scan Line Corrector failure, which occurred in 2003. We used Spectral bands 5, 4 and 3 to highlight ice contacts [Quinn, 2001]. Imagery was pan-sharpened with band 8, increasing the resolution from 30 to 15 m. We also used ASTER Global Digital Elevation Models accessed through the United States Geological Survey's EarthExplorer database in glacier delineation [Farr et al., 2007]. This elevation model has a 1 arc-second resolution which roughly translates to 30 m. Finally, we referenced the Google Earth Pro (v7.3.2.5491, Google) satellite image database to aid in glacier delineation. Annual rainfall averages were obtained from 4000 m resolution TRMM satellite data [Bookhagen, in review; http://www.geog.ucsb.edu/~bodo/TRMM/]. The annual averages represent 12 years of data.

3.2. Glacier data

446 Glaciers were mapped in Arcmap (v10.4, ESRI) based on observations of Landsat, GDEM, and GoogleEarth imagery and data, along with slope maps generated from GDEM data.

Although automated methods exist, we prefer in this study to map glaciers manually because of the extreme variation in debris cover and the frequency of steep, shadowed headwalls.

Glacier mapping was straightforward for debris-free glaciers with well-defined headwall bergschrunds. Mapping was aided by DEM-derived slope maps; glaciers typically have uniformly low surface slopes due to the ductile properties of glacier ice [Hudleston, 2015], therefore contacts between regions of high and low slope often mark glacier margins. For glacier boundaries near the head wall, the contact between glacier ice and the head scarp was used, sometimes marked by a bergschrund or by a contrast between cleaner glacier ice, and streaky headwall ice and debris with rocky outcroppings. In cases in which the entire head scarp is snow- or shadow-covered, we mapped glaciers using contrast visible on the slope map. Where lateral moraines were present, we mapped the glacial margin at the inside edge of the moraine, often marked by erosion based "hatch" lines perpendicular to the glacier boundary. For boundaries near the toe of the glacier, particularly with significant debris cover, the contact between glacier ice and terminal lakes was used. For glaciers without terminal lakes, we used the contact between glacier ice and outflowing rivers. Given the debris cover and the low contrast in slopes between the glacier and the surrounding region, our mapping in the toe region is most uncertain. Glaciers in similar geomorphic locations were given a zoning label.

We constructed a glacial center-line, and identified a center- and peak-point for each glacier. The glacial center-lines were created by connecting the highest to lowest elevation points through the path of expected glacial flow. Center-points were placed on the midpoint of glacial flow (often on the center-line), roughly at the snowline (we did not use the polygon centroid as it is possible for it to lie outside a glacier with a curved or convoluted geometry). Peak-points were identified as the highest points of elevation nearest to each glacier. Adjacent glaciers often shared peak-points. Spatial joins were used to join the features of the center-line, center-point and peak-point. Non-spatial joins were used to join the ASTER GDEM, Slope and TRMM data. The resulting database allows for spatial and non-spatial correlation of key glacier attributes (Table 1).

4. Results

4.1. Glaciers

We mapped a total of 446 ice-glaciers in the Dolpo region, assigning them to four regional clusters. The largest concentration of glaciers is in the southern region, with 172 mapped glaciers. The northern and western regions encompass 104 and 130 glaciers respectively. The eastern region is sparsest, with only 40 mapped glaciers. Only 110 of the 446

Table 1
Key glacier attributes in the study region.

Glacier attributes	Attribute definition and source
Glacier area	Area of glacier outline in kilometers^2
Glacier length	Length of glacier center-line in kilometers
Glacier slope	Calculated from length, head, and toe elevation in degrees: $Slope = (HeadElevation - ToeElevation)/Length$
Centerpoint X	UTM (44N) centerpoint coordinates
Centerpoint Y	UTM (44N) centerpoint coordinates
Peak elevation	Elevation of the topographic peak nearest each glacier in meters
Peak distance	Closest distance from glacier outline to peak-point in meters
Head elevation	Highest elevation in the glacier polygon in meters
Toe elevation	Lowest elevation in the glacier polygon in meters
Average elevation	Average elevation of the glacier polygon in meters
Precipitation max	Max precipitation value intersecting glacier polygon in mm/year
Aspect	Compass direction of the glacial flow from the head to toe in degrees

mapped glaciers lie within the boundaries of the Dolpo drainage basin. The rest lie within the ranges that bound the basin, but outside of the drainage divide.

We found a strong linear correlation between glacier length and area (Fig. 3a). Regional slope has a negative non-linear relationship with glacier length (Fig. 3b), while peak elevation has a positive non-linear relationship (Fig. 3c). Interestingly, precipitation does not correlate with peak elevation (Fig. 3d), nor glacier length (Fig. 3e); however, precipitation does have a strong positive linear correlation with glacier slope (Fig. 3f). Glaciers that are located in the eastern part of Dolpo basin have lower maximum slopes than those to the west (Fig. 3g). Northern glaciers north of the divide are longer than those south of the divide and within the basin (Fig. 3h). Finally, we observe cardinal biases on glacier size, with the longest glaciers flowing toward the northeast (Fig. 3i).

4.2. Regional slope

Slope varies significantly within the study region (Fig. 4). The western part of the basin, near its outlet, has an average slop that exceeds 30°. In contrast, the eastern portion of the basin has an average slope of 20°-30°, and the Tibetan plateau, north of the basin, has an average slope <20°. Correlations to river steepness [Cannon and Murphy, 2014] are explored in the discussion.

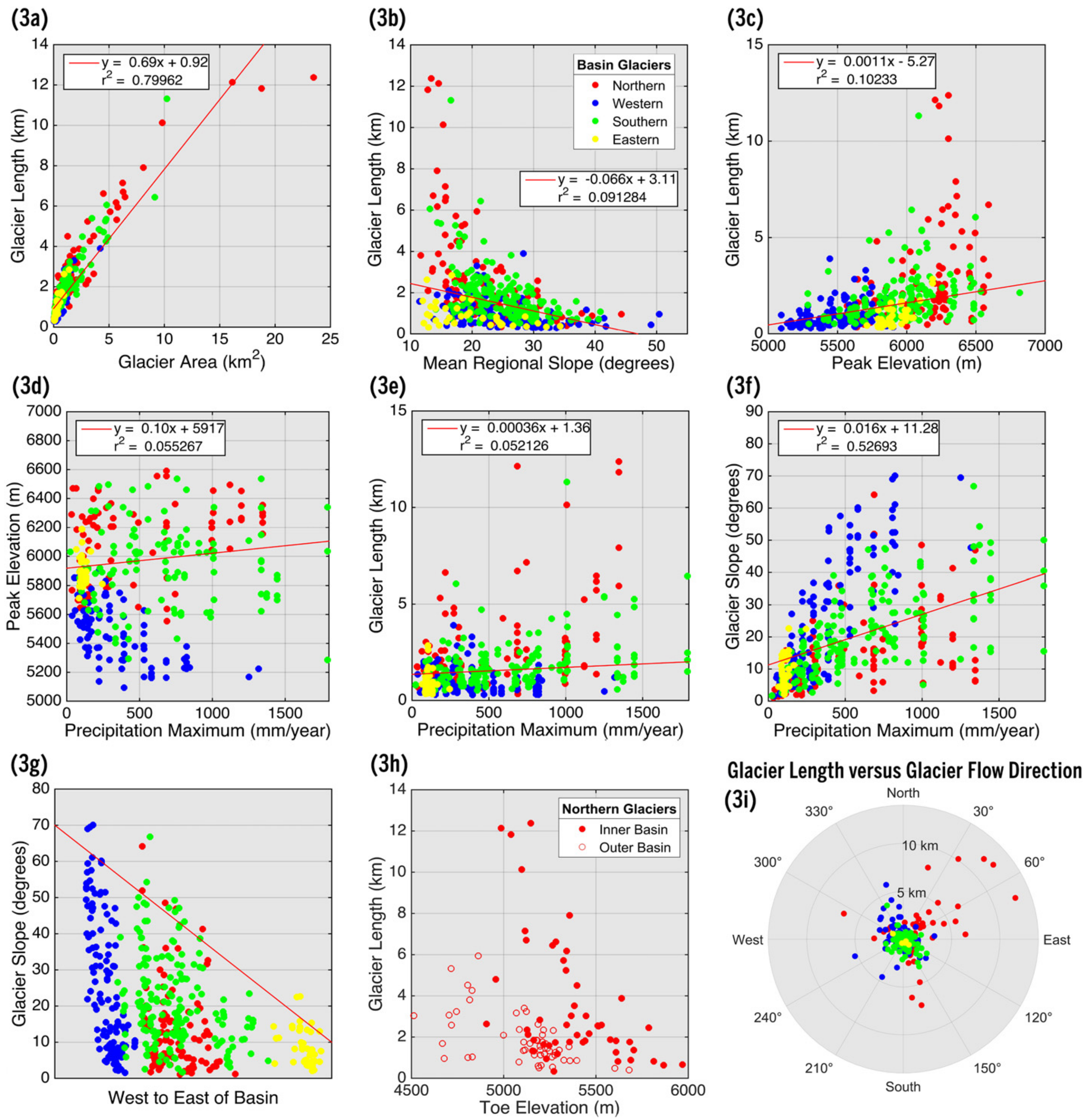

Fig. 3. Graphs of several glacial statistics plotted against one another with sub-figure labels at their upper left corners. All graphs, except for Fig. 3h, utilize the legend in Fig. 3b.

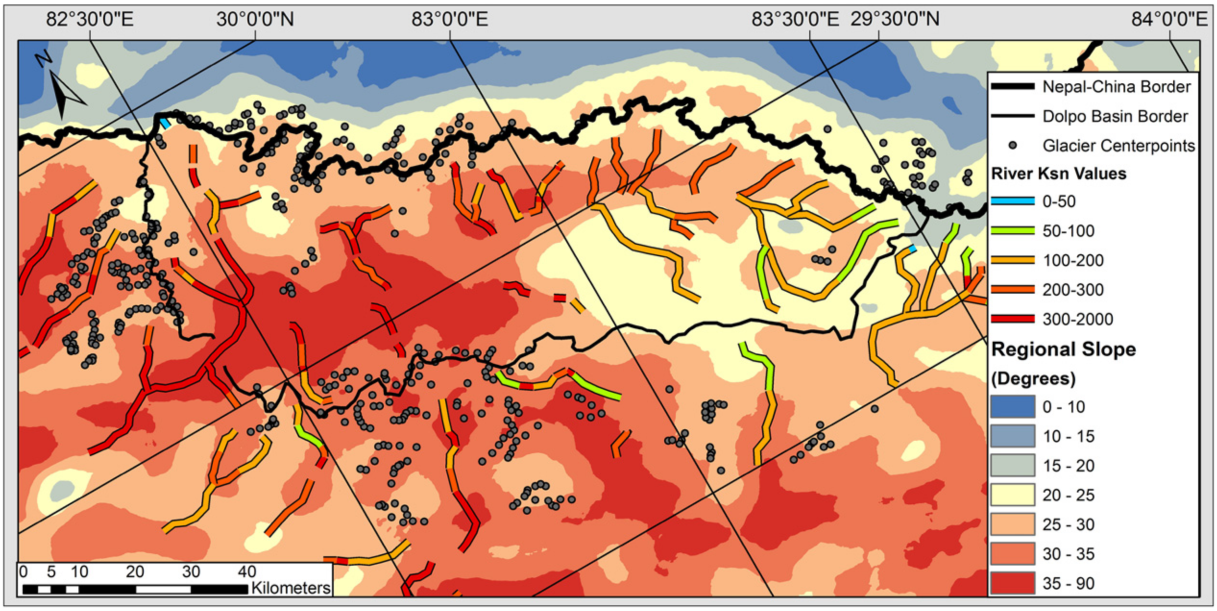

Fig. 4. Slope map of the Dolpo basin. Slope is smoothed using 4000 m radius moving window. Channel steepness (k_{sn}) from Cannon and Murphy (2014). Note the correlation of slope and steepness, and the higher values of both near the basin outlet in the west.

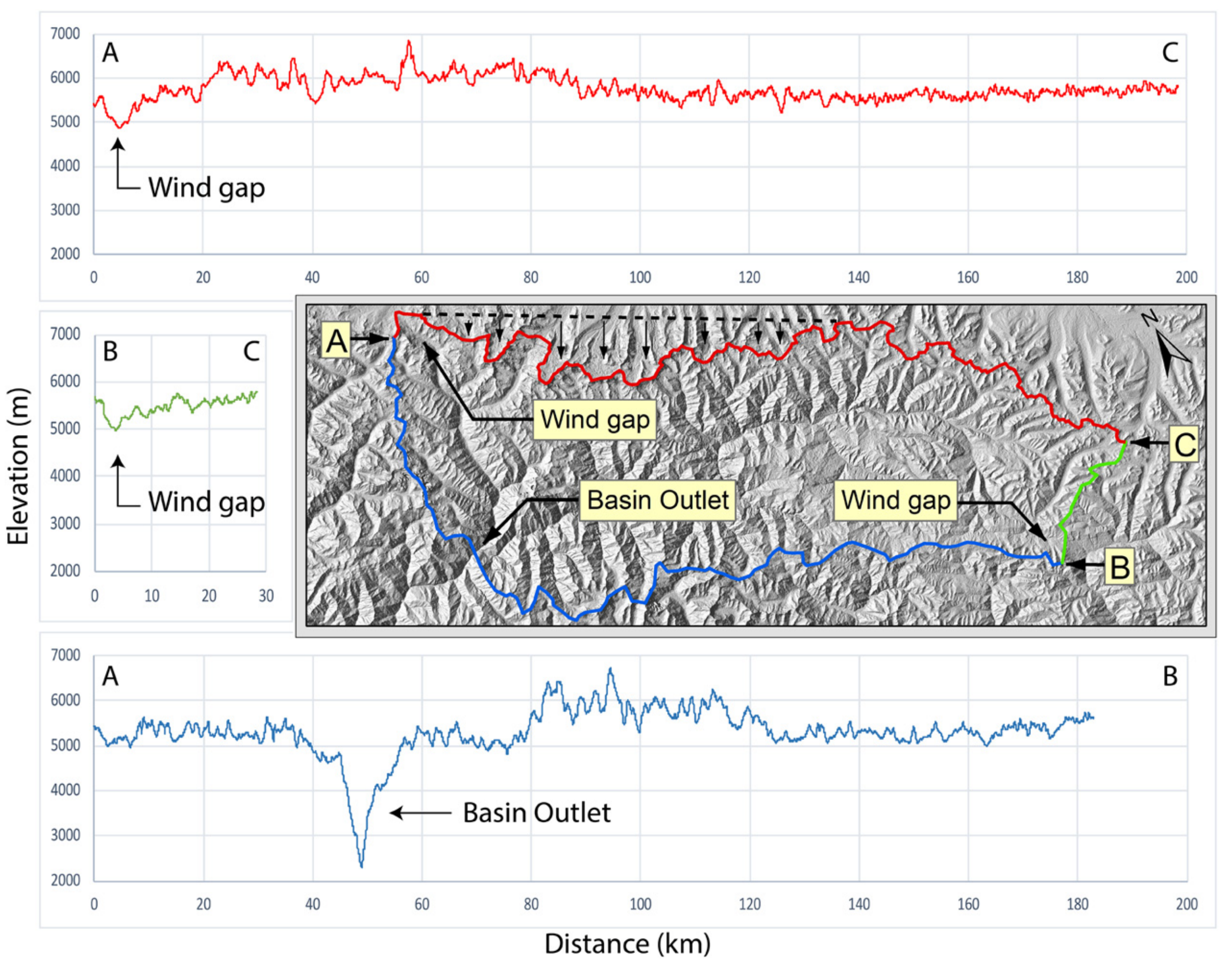

Fig. 5. Elevation profiles along the basin's drainage borders. Locations of significant low points in the divide on profiles AC and BC are highlighted – these are wind gaps. Modern basin outlet is indicated on profile AB. Dashed black line on map illustrates supposed original orientation and position of the northern drainage divide; arrows originating from this line indicate places where the divide is has migrated southward.

4.3. Basin geomorphology

A number of geomorphic features within the study area are noteworthy. The northern border of the basin is sinuous, bulging southward into the basin near the eastern and western ends of the basin, but bulging northward along the center of the northern divide with a wavelength of roughly ~110 km and an amplitude of 5–10 km (Fig. 5). We also observe several significant potential wind gaps (abandoned stream channels) along the Dolpo basin's drainage divide. A wind gap at the western end of the northern drainage border drops to an elevation of 4890 m while the average elevation of the northern basin border is ~6000 m. A second wind gap near the southernmost point along the eastern drainage divide drops to an elevation of 5017 m while the average elevation of the eastern basin border is ~5500 m.

4.4. Basin precipitation

The Dolpo basin receives highly variable precipitation (Fig. 6). South of the basin, precipitation reaches 900+ mm/year, but rates drop sharply to the northeast, becoming negligible within the Tibetan plateau. Precipitation is greater in the western part of the Dolpo basin, particularly near the outlet of the basin and near the western parts of the northern and southern basin borders. The eastern part of the basin receives less yearly precipitation.

5. Discussion

5.1. Glacier dynamics

Numerous studies have shown glaciers to be sensitive to variations in climate, topography, and aspect [e.g., Kayastha and Harrison, 2008; Pratt-Sitaula et al., 2011; Scherler et al., 2011]. However, the glaciers in our study run contrary to some of the results of previous studies in several ways which we explore below.

Glaciers vary significantly in size throughout the Dolpo basin – we measure this variation through glacier length, which exhibits correlations with other glacier characteristics (e.g., Fig. 3a, b, c and h). In other studies [e.g., Hannah et al., 2005; Anders et al., 2006], peak elevation and precipitation have been found to correlate, suggesting that peaks act as "tectonic lightning rods", attracting orographic precipitation, which feeds surrounding glaciers. High peaks can also act to shade glaciers, promoting growth particularly on north and northeastern slopes in the northern hemisphere [Evans, 1977]. We do find a non-linear positive correlation between peak elevation and glacier length, such that higher topographic peaks are associated with longer glaciers (Fig. 3c). However, there is no correlation between precipitation and glacier length (Fig. 3e), and no correlation between precipitation and peak elevation (Fig. 3d). This could reflect the low resolution of available precipitation data (~40 km grid vs. ~30 m topographic grid), or the importance of other factors in promoting glacier growth.

Our data suggest that glacier base-level is an important and often overlooked factor in setting glacier morphology through two mechanisms. First, if base-level is forced to a relatively high elevation, as would be the case for glaciers flowing onto any high-elevation surface that resides above or close to the ELA, the majority of the area of the glacier will also reside above or close to the ELA, thus promoting glacier growth. Indeed, we see a non-linear correlation between glacier slope and length (Fig. 3b), and between toe elevation and glacier length for northern basin glaciers (Fig. 3h). The largest glaciers near the Dolpo basin are those that flow directly northward off of the northern basin divide onto the Tibetan plateau, spreading out across a large area at or just below the ELA, despite relatively low precipitation. Shading may play a role here as well, as glaciers north of the border face northeast (Fig. 3i), although we don't observe aspect-related trends in other regions of the study area, meaning it is likely not a major contributing factor.

If a high base-level has positive effects on glacier size, a low base-level has the opposite effect, partly because steeper glacier slopes mean that of less of a glacier will reside above the ELA, but also likely because glaciers can become disaggregated and have difficulty retaining their corporeality on steep hillslopes (Fig. 3b). Glaciers south of the divide in this region tend to be avalanche, rather than direct-snowfall fed [Scherler et al., 2011]. We find that precipitation (presumably in the form of snow) and glacier slope have a strong linear correlation (Fig. 3f), suggesting that areas of high precipitation can still support glaciers in areas of high relief, thus compensating for the negative effects of steep hillslopes and a low base-level. In other words, high precipitation can force glaciation in areas of steep regional terrain that would otherwise not be able to support glaciation (Fig. 6).

There are spatial trends in glacier slope and length across our study region. As previously noted, the largest glaciers lie along the northern

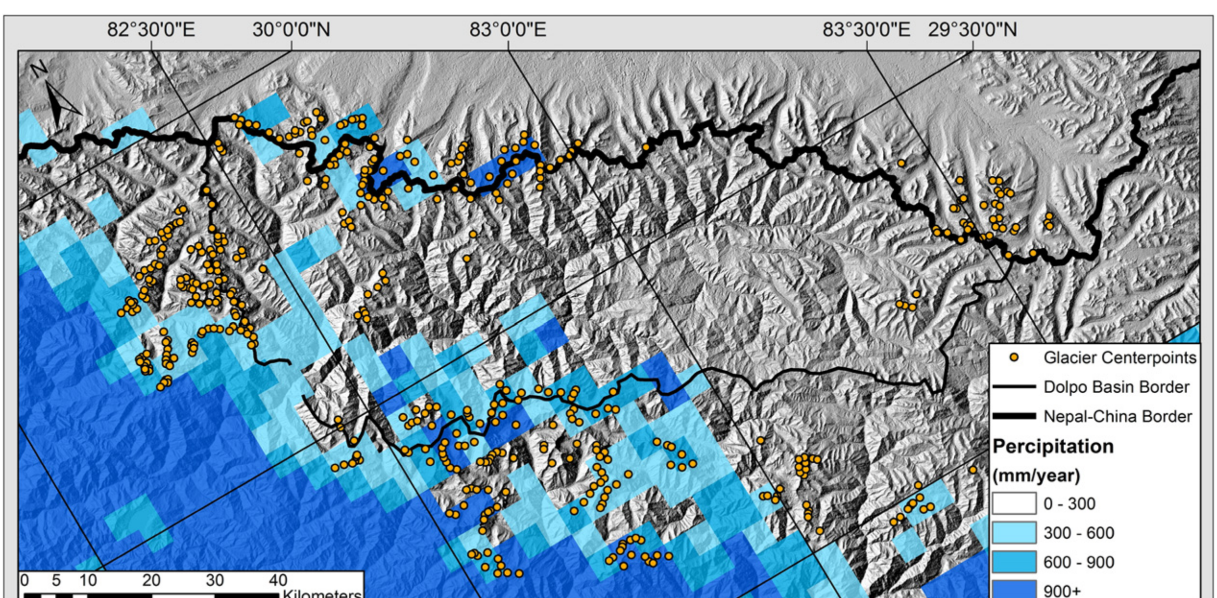

Fig. 6. Precipitation map of the Dolpo basin from TRMM satellite data, processed by Bookhagen (in review). Note higher precipitation values near basin outlet and at western end of northern basin border.

side of the northern border of the basin, with their base-level set by the high (~5000 m) elevations of the upper Yarlung River basin (Figs. 1 and 5). Within the Dolpo basin, glacier slopes are steeper in the west than in the east (Fig. 3g), with steepest slopes concentrated near the outlet of the basin (Fig. 4). This suggests recent base-level lowering within the Dolpo basin, particularly focused near the basin outlet, an observation that we explore below as we develop a model for the landscape development of this region.

As has been found in other studies [e.g., Schoenbohm et al., 2014; Ward et al., 2012], glaciers have a complex relationship with lithology and with spatial variation in precipitation. Glaciation appears to be restricted to certain lithologies (Fig. 2). There are no glaciers in the entire study area within TSS sedimentary rocks; glaciers are found only within TSS metasedimentary rocks, GHS rocks, and leucogranites. Particularly illustrative is a small cluster of glaciers on an isolated outcrop of leucogranite within TSS sedimentary rocks in the eastern part of the basin (Fig. 2). It is possible that fluvial or prior glacial erosion has eroded the weaker TSS sedimentary rocks down to elevations below the threshold to support modern glaciers. However, this hypothesis is only partly supported by observations, as elevations are slightly lower in the region underlain by TSS sedimentary rocks, but high peaks still exist throughout this region (compare Figs. 2 and 7). The question of why TSS sedimentary units do not support glaciers is thus unresolved. Interestingly, although a weak lithology might preclude glaciation in the Dolpo basin, a strong lithology does not ensure it, as is particularly striking along the northern border of the basin which is heavily glaciated to the west and east, but unglaciated along its middle portion despite identical lithology and high elevations (Figs. 2 and 5). This observation points back to precipitation as an important factor, not so much for glacier size, but for the presence or absence of glaciers. The only portion of the northern basin border that receives substantial precipitation is the western end, which may explain the presence of large glaciers there, in contrast to the absence of glaciers in the central arid section of the northern border (Fig. 2). The origin of the glaciers on the eastern end of the northern border is enigmatic, as that area is also largely arid.

Finally, we observe sinuosity in the position of the ridgeline of the northern border of the basin, with it positioned to the south in the western and eastern portions of the basin where glaciers are abundant, and positioned to the north in the center of the northern basin border, where glaciers are absent (Figs. 1 and 5). Glaciers on the northern side of the border tend to be larger as well, owing to their high base-level (Fig. 3h), and possibly also because of shading due to their northeast aspect (Fig. 3i); although the direct effects of shading are restricted to areas close to glacier headwalls, because this is a critical location for accumulation of snow and ice, the shading effect can be significant [Evans, 1977]. We suggest that the large, northern glaciers eroded their headwalls southward, over time offsetting the ridgeline by up to about 20 km, as has been observed in other studies [e.g., Foster et al., 2010; Dortch et al., 2011; Schoenbohm et al., 2014].

In summary, our data suggest that glacier size is sensitive to peak elevation and to a lesser extent precipitation, but that hillslope and base-level are stronger predictors of glacier size. The spatial distribution of glaciers is controlled by lithology, precipitation, and hillslope. In the next section we present a landscape model to explain regional phenomena, such as variations in glacier slope and therefore base-level within the Dolpo basin, precipitation patterns across the basin, and the sinuosity of the northern border of the basin.

5.2. Landscape evolution model

We hypothesize a landscape evolution model to explain glacier and other geomorphic features of the Dolpo basin. In this model, the Dolpo basin originally drained northward into the Yarlung River basin. Northward drainage from the Dolpo basin was then captured or diverted to the south. This capture caused a wave of incision, forced by the sudden drop in fluvial base-level, to work its way into the basin, progressively forcing the base-level for glaciers within the Dolpo basin to drop as well. The new southern river valley allowed precipitation to enter the Dolpo basin, enhancing inner-basin glaciation. We outline the evidence for and implications of this model below, while also testing the null hypothesis of drainage basin antecedence, where the basin has undergone these changes without drainage capture.

We derive evidence for the drainage capture of the Dolpo basin using observations of geomorphic features within the basin. We observe a ~1000 m deep wind gap in the drainage divide between the Tibetan plateau and Nepal in the northernmost corner of the Dolpo basin (Fig. 5). This wind gap suggests that there had once been drainage between the Tibetan plateau and Nepal; although, the direction of drainage can only be inferred from other geomorphic features without ground-based observations. We observe a second wind gap (Fig. 5),

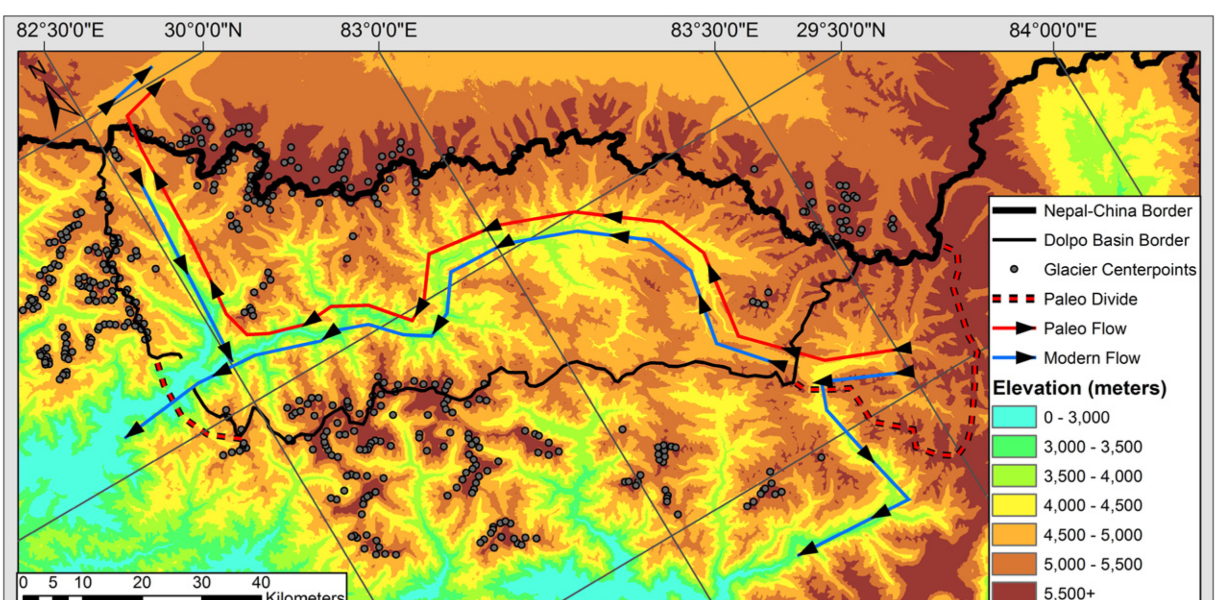

Fig. 7. Model for the evolution of the Dolpo basin. The basin originally drained northward onto the Tibetan plateau but was diverted or captured to the south, into the Karnali River drainage basin. Note the additional small capture east of the basin.

marked by a ~500 m decrease in average elevation along the ridgeline on the eastern margin of the Dolpo basin. This second wind gap suggests that the Dolpo basin once extended farther east, but the eastern most portion of the basin was captured from the south by a southward flowing drainage, possibly in the headwaters of the Thulo Bheri or Kaligandaki Rivers (Fig. 7). There is also a significant disparity between the relief of the western and eastern parts of the Dolpo basin. Steep hillslopes are concentrated near the outlet of the Dolpo basin and shallower hillslopes are found in the basin interior to the east; these regions are strongly demarcated by a shift in regional relief (Fig. 4). River steepness (k_{sn}) shows a similar pattern, with high k_{sn} rivers in the west near the basin outlet and low k_{sn} values along rivers in the east (Fig. 4) [Cannon and Murphy, 2014]. Glacier slope also follows this trend, with steepness decreasing from west to east (Fig. 3g). This longitudinal change in hillslope suggests that the Dolpo basin is being actively incised. The change in relief within the basin likely represents an incisional front caused by a sudden change in fluvial base-level. We attribute this change to southward drainage capture by the westward flowing Mugu Karnali tributary of the Karnali River. This capture has previously been suggested by Brookfield (1998). The base-level for both fluvial and glacial processes within this basin has since dropped from ~3500 m (Yarlung River) to ~2300 m (modern Dolpo basin outlet).

In the antecedent river model, wind gaps found within the drainage basin could be a product of glacier erosion, with a now extinct glacier having breached the drainage divide through the erosion of its headwall. This phenomenon can produce low spots in a ridgeline; however, the magnitude of the elevation drop in this case suggests a fluvial origin. The wind gaps could also be the product of now-extinct southward flowing paleo trans-Himalayan rivers rather than our proposed northward flowing rivers. Without ground-based observations of paleo-flow direction, we cannot rule out this possibility. It is also possible for a similar incisional front to occur without a drainage capture. This could be accomplished through either uplift of the Dolpo basin or a significant base-level drop along the Karnali River. However, a rapid base-level drop of 2000 m in the southern Himalayan foothills is highly unlikely and not suggested by any existing studies. Ultimate local base-level for the Karnali River is the northern part of the Gangetic foreland basin, which has remained at approximately its modern (~100–200 m) elevation since middle Miocene time [Quade et al., 1995; DeCelles et al., 1998]. Recent uplift within the Dolpo basin, suggested by Cannon and Murphy (2014), is also not shown by any existing studies. Vertical velocity rates of the eastern inner portions of the Dolpo basin are negligible [Grandin et al., 2012]. Uplift models of central Nepal derived from interseismic deformation [Cattin and Avouac, 2000] and from fluvial incision [Lave and Avouac, 2001] show significant uplift along the MCT, 20–50 km south of the Dolpo basin (Fig. 2) rather than within the Dolpo basin. In summary, although we cannot completely rule out a glacial or north-flowing river origin for the wind gaps, taken along with other evidence for capture of the Dolpo basin to the south, we find support for our landscape evolution model.

Opening of the Dolpo basin to the south would have had a significant impact on the distribution of precipitation within the basin. Prior to capture, a major southern basin divide would have intercepted northbound monsoon moisture, preventing appreciable precipitation from reaching the northern basin divide. However, capture would have opened a pathway through the high peaks and ridgeline south of the basin, analogous to the opening of the Manang basin north of the Annapurna Range by the Marsyangdi River in central Nepal [e.g., Bookhagen et al., 2005], allowing moisture to penetrate along the river valley, reaching the western part of the northern basin border (Fig. 6). This post-capture pattern of precipitation explains the modern location of major glaciers along the northern border of the basin (Fig. 2), and in fact implies that the minimum age of basin capture could be dated by dating the onset of glaciation along the Tibet-Nepal border; regionally synchronous onset of glaciation, in contrast, would support the antecedent river model – such a test will have to wait for a future study. A similar story may have unfolded to the east, with the capture of the southernmost part of the Dolpo basin also opening up a pathway for precipitation to reach the eastern part of the northern basin border (Fig. 6) although here the pathway is less clear, and modern precipitation values are low.

Capture could have been driven by uplift to the north cutting off drainage onto the Tibetan plateau, by capture of south-flowing, headward-eroding tributaries to the Karnali River, or a combination of both. Uplift north of the Dolpo basin is likely; a band of antiformal leucogranites marks the northern border of the modern Dolpo basin (Fig. 2), and although there is no apparent uplift of this range today [Grandin et al., 2012], uplift may have occurred in the past by underthrusting of LHS units below GHS units [Beaumont et al., 2001; Cannon and Murphy, 2014], causing doming and eventually exhumation of leucogranites (Figs. 2, 8). This is possible due to high relative shortening rates in this region [Robinson et al., 2006; Bhattacharyya and Ahmed, 2016] and the low regional plate coupling strength [Ader et al., 2012; Jouanne et al., 2017]. Uplift could have been progressive, restricting flow from the Dolpo basin to a single channel cutting through the range at the northern end of the modern Dolpo basin, until that finally was defeated. In this scenario, the Dolpo basin could have temporarily experienced internal drainage [e.g., Saylor et al., 2010], although no confirming lacustrine sediments have been identified. At some point, either through northward incision along the Mugu Karnali River, or overtopping of the divide separating the closed Dolpo basin from the Karnali watershed, the divide was breached. Headward erosion is likely to be faster than isotactic uplift in this region, suggesting that the former mechanism occurred [Brookfield, 1998].

Our observation of a wave of incision and glacial steepening moving through the Dolpo basin supports the landscape evolution model over the antecedent model. Combined geomorphic and glacial observations suggest that the Dolpo basin once belonged to geomorphic Tibet (the Tibetan plateau), with drainage flowing generally northward into the Yarlung River watershed. Our study thus lends credence to the idea that the Tibetan landscape once extended a large distance to the south in the Everest region during the mid-Miocene, prior to fluvial incision during the Pliocene [Carrapa et al., 2016].

6. Conclusion

In this study, we investigated the glacial and geomorphic characteristics of a region in northern Dolpo which we refer to as the Dolpo basin. We cataloged 446 glaciers in and near this basin and found spatial and non-spatial trends among our glacier population. The elevation of peaks near glaciers correlated positively with glacier size, but contrary to other studies, we find no distinct correlation between peak elevation and precipitation. Taller peaks imply larger head and side walls over which snow and ice can accumulate, contributing to development of larger glaciers. Our data also highlight the often-overlooked factor of base-level in determining glacier size. Glaciers that are forced to an overall high elevation by a high base-level, like those that flow northward off of the northern Dolpo basin divide, are likely larger because more of the glacier area is forced to be at or above the ELA. Glaciers are spatially correlated with lithology, absent on TSS sedimentary units and present on TSS metasedimentary, GHS, and leucogranite units. This we attribute to lithologic strength, with weaker TSS rocks eroded to an elevation below the ELA, rendering glaciation impossible. Although we observe a low correlation between precipitation and glacier size, we observe a strong spatial clustering between the density of glaciation and high precipitation.

The distribution of hillslope and river steepness in the Dolpo basin, along with presence of a wind gap to the north of the basin support a landscape evolution in which the basin once drained

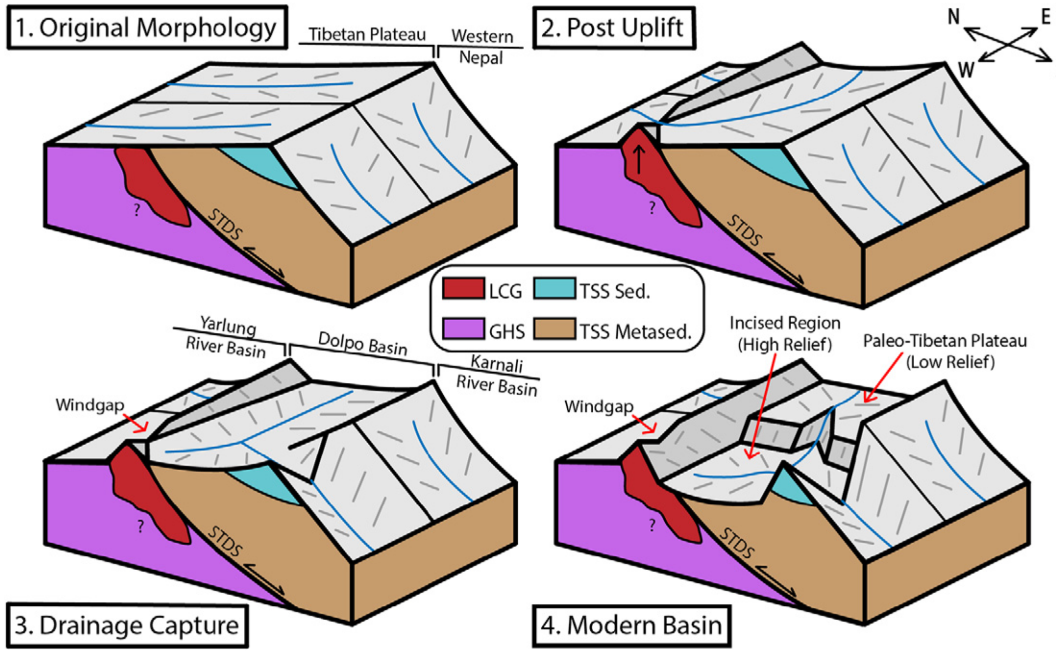

Fig. 8. Schematic representation of the Dolpo basin illustrating the proposed landscape evolution model. The TSS units in this region are folded, forming a syncline which extends further south. North of this syncline are a band of antiformal leucogranites which form the northern border of the Dolpo basin. Southward capture of the basin led to a base-level drop which drove incision into the basin, creating both regions of high and low reliefs. This drainage capture also led to the preservation of temporary northward flow as a wind gap. STDS = South Tibetan Detachment System, LGN = Miocene leucogranite, GHS = Greater Himalayan Sequence, TSS = Tethyan Sedimentary Sequence, Sed = Sedimentary Rocks, Metased = Metasedimentary Rocks.

northward onto the Tibetan plateau. After capture or diversion of the basin, the drop in base-level would have caused incision and steepening progressively from the capture point. This westward and southward capture created a pathway for precipitation to enter into the basin, likely causing the establishment of glaciers at the northwestern end of the northern drainage border. A similar wind gap exists to the south of the basin implying that the basin had once extended eastward before a similar southward capture. Differential base-level along the northern border likely drives asymmetrical glacial erosion, forcing the basin border to migrate south in glaciated areas. This capture model implies that low-relief, high elevation Tibetan landscape once extended a minimum of 45 km southward in the Dolpo region. This northern Dolpo area features dynamic coupling of complex geomorphological, glacial and tectonic controls. Much has yet to be discovered or fully understood in this region, but the findings of this study point to its importance in the recent geologic and geomorphic evolution of the western Nepal Himalayas.

Declaration of competing interest

The authors declare that they have no known competing financial interests or personal relationships that could have appeared to influence the work reported in this paper.

Acknowledgements

This work was supported by a Natural Sciences and Engineering Research Council of Canada (NSERC) Discovery grant to Lindsay Schoenbohm (University of Toronto), an NSERC Undergraduate Summer Research Awards (USRA) to Rhys Buceta, and the US NSF-Tectonics Program (grant EAR1763432). All data are contained in this manuscript.

Data availability

Datasets related to this article can be found at: https://data.mendeley.com/datasets/98k5vs6mb2/draft?a=09348481-c9a5-423c-97d1-e15f841363f6], hosted at Mendeley Data ([Buceta and Schoenbohm, 2020]).

References

Adams, B.A., Whipple, K.X., Hodges, K.V., Heimsath, A.M., 2016. In situ development of high-elevation, low-relief landscapes via duplex deformation in the eastern himalayan hinterland, bhutan. Journal of Geophysical Research: Earth Surface 121 (2), 294–319. https://doi.org/10.1002/2015JF003508.

Ader, T., Avouac, J., Liu-Zeng, J., Lyon-Caen, H., Bollinger, L., Galetzka, J., Flouzat, M., 2012. Convergence rate across the Nepal Himalaya and interseismic coupling on the Main Himalayan Thrust: implications for seismic hazard. Journal of Geophysical Research: Solid Earth 117 (4). https://doi.org/10.1029/2011JB009071.

Anders, A. M., Roe, G. H., Hallet, B., Montgomery, D. R., Finnegan, N. J., Putkonen, J., 2006. Spatial patterns of precipitation and topography in the Himalaya. Geological Society of America, Special Papers, 398. doi:10.1130/2006.2398(03).

Beaumont, C., Jamieson, R.A., Nguyen, M.H., Lee, B., 2001. Himalayan tectonics explained by extrusion of a low-viscosity crustal channel coupled to focused surface denudation. Nature 414 (6865), 738–742. https://doi.org/10.1038/414738a.

Bertoldi, L., Massironi, M., Visonà, D., Carosi, R., Montomoli, C., Gubert, F., Pelizzo, M.G., 2011. Mapping the Buraburi granite in the Himalaya of western Nepal: remote sensing analysis in a collisional belt with vegetation cover and extreme variation of topography. Remote Sens. Environ. 115 (5), 1129–1144. https://doi.org/10.1016/j.rse.2010.12.016.

Bhattacharyya, K., Ahmed, F., 2016. Role of initial basin width in partitioning total shortening in the Lesser Himalayan fold-thrust belt: insights from regional balanced cross-sections. J. Asian Earth Sci. 116, 122–131. https://doi.org/10.1016/j.jseaes.2015.11.012.

Bookhagen, B., 2020. High Resolution Spatiotemporal Distribution of Rainfall Seasonality and Extreme Events Based on a 12-Year TRMM Time Series. (in review)

Bookhagen, B., Thiede, R.C., Strecker, M.R., 2005. Abnormal monsoon years and their control on erosion and sediment flux in the high, arid northwest Himalaya. Earth Planet. Sci. Lett. 231 (1–2), 131–146. https://doi.org/10.1016/j.epsl.2004.11.014.

Brookfield, M.E., 1998. The evolution of the great river systems of southern Asia during the Cenozoic India-Asia collision: rivers draining southwards. Geomorphology 22 (3–4), 285–312. https://doi.org/10.1016/S0169-555X(97)00082-2.

Brocklehurst, S.H., Whipple, K.X, 2002. Glacial erosion and relief production in the eastern sierra nevada, california. Geomorphology 42 (1-2), 1–24. https://doi.org/10.1016/S0169-555X(01)00069-1.

Buceta, Rhys E., Schoenbohm, Lindsay M., 2020. "Glacial and fluvial erosion in the Dolpo Basin, Western Nepal DATA". Mendeley Data, v1 https://doi.org/10.17632/98k5vs6mb2.2.

Burchfiel, B.C., Zhiliang, C., Hodges, K.V., Yuping, L., Royden, L.H., Changrong, D., Jiene, X., 1992. The South Tibetan Detachment System, Himalayan Orogen: Extension Contemporaneous With and Parallel to Shortening in a Collisional Mountain Belt. Geological Society of America, Special Papers, p. 269.

Burg, J.P., Brunel, M., Gapais, D., Chen, G.M., Liu, G.H., 1984. Deformation of leucogranites of the crystalline Main Central Sheet in southern Tibet (China). J. Struct. Geol. 6, 535–542. https://doi.org/10.1016/0191-8141(84)90063-4.

Cannon, J.M., Murphy, M.A., 2014. Active lower crustal deformation and Himalayan seismic hazard revealed by stream channels and regional geology. Tectonophysics 633, 34–42. https://doi.org/10.1016/j.tecto.2014.06.031.

Carosi, R., Montomoli, C., Rubatto, D., Visonà, D., 2010. Late Oligocene High-temperature Shear Zones in the Core of the Higher Himalayan Crystallines (Lower Dolpo, Western Nepal), 29, TC4029. https://doi.org/10.1029/2008TC002400.

Carrapa, B., Robert, X., DeCelles, P.G., Orme, D.A., Thomson, S.N., Schoenbohm, L.M., 2016. Asymmetric exhumation of the Mount Everest region: Implications for the tectono-topographic evolution of the Himalaya. Geology 44 (8), 611–614. https://doi.org/10.1130/G37756.1.

Cattin, R., Avouac, J.P., 2000. Modeling mountain building and the seismic cycle in the Himalaya of Nepal. Journal of Geophysical Research: Solid Earth 105 (B6), 13389–13407. https://doi.org/10.1029/2000JB900032.

Clark, M.K., Schoenbohm, L.M., Royden, L.H., Whipple, K.X., Burchfiel, B.C., ... Zhang, X., 2004. Surface uplift, tectonics, and erosion of eastern tibet from large-scale drainage patterns. Tectonics 23 ((1), 1–20. https://doi.org/10.1029/2002TC001402 TC1006.

DeCelles, P.G., Gehrels, G.E., Quade, J., Ojha, T.P., Kapp, P.A., Upreti, B.N., 1998. Neogene foreland basin deposits, erosional unroofing, and the kinematic history of the Himalayan fold-thrust belt, western Nepal: Geological Society of America Bulletin, 110, 2–21. https://doi.org/10.1130/0016-7606(1998)110<0002:NFBDEU>2.3.CO;2.

Dortch, J.M., Owen, L.A., Schoenbohm, L.M., Caffee, M.W., 2011. Asymmetrical erosion and morphological development of the central Ladakh range, northern India. Geomorphology 135 (1–2), 167–180. https://doi.org/10.1016/j.geomorph.2011.08.014.

Duncan, C.C., Klein, A.J., Masek, J.G., Isacks, B.L., 1998. Comparison of late pleistocene and modern glacier extents in central Nepal based on digital elevation data and satellite imagery. Quat. Res. 49 (3), 241–254. https://doi.org/10.1006/qres.1998.1958.

Evans, I.S., 1977. The geomorphology and morphometry of glaciated mountains. In: Chorley, R.J. (Ed.), Water, Earth and Man. Methuen, London, pp. 369–380.

Farr, T.G., et al., 2007. The shuttle radar topography mission. Rev. Geophys., 45, RG2004. doi: 10.1029/2005RG000183.

Foster, D., Brocklehurst, S.H., Gawthorpe, R.L., 2010. Glacial-topographic interactions in the Teton Range. Wyoming. J. Geophys. Res. 115, F01007. https://doi.org/10.1029/2008JF001135.

Frank, W., Fuchs, G.R., 1970. Geological investigations in west Nepal and their significance for the geology of the Himalayas. Geol. Rundsch. 59 (2), 552–580. https://doi.org/10.1007/BF01823808.

Fuchs, G., 1964. Beitrag zur Kenntnis des Palaozoikums und Mesozoikums der Tibetischen Zone in Dolpo (Nepal Himalaja). Sonderabdruck aus den Verhandlungen der Geologischen Bundesanstalt 1, 6–9.

Fuchs, G., 1967. Zum Bau des Himalaya. Denkschr. Osterr. Akad. Wiss., math.-naturw. 113, 1–211.

Fuchs, G., 1973. On the Geology of the Karnali and Dolpo Regions, West Nepal. Mitteilungen der Geologischen Gesellschaft in Wien 66–67, 21–32.

Fuchs, G., 1977. The geology of the Karnali and Dolpo regions. Western Nepal. Jahrbuch der Geologischen Bundesanstalt Band 120 (2), 165–217.

Fuchs, G., Frank, W., 1970. The geology of west Nepal between the rivers Kali Gandaki and Thulo Bheri. Jahrb. Geol. Bundesanst. 18, 103.

Fuchs, G., Poudel, L.P., 1998. Note on the Tethyan sedimentary series of the Manaslu region (northern Nepal). Jahrb. Geol. Bundesanst. 141, 45–50.

Grandin, R., Doin, M., Bollinger, L., Pinel-Puysségur, B., Ducret, G., Jolivet, R., Sapkota, S.N., 2012. Long-term growth of the Himalaya inferred from interseismic InSAR measurement. Geology 40 (12), 1059–1062. https://doi.org/10.1130/G33154.1.

Hannah, D.M., Kansakar, S.R., Gerrard, A.J., Rees, G., 2005. Flow regimes of Himalayan rivers of Nepal: nature and spatial patterns. J. Hydrol. 308 (1–4), 18–32. https://doi.org/10.1016/j.jhydrol.2004.10.018.

Harvey, J.E., Burbank, D.W., Bookhagen, B., 2015. Along-strike changes in Himalayan thrust geometry: topographic and tectonic discontinuities in western Nepal. Lithosphere 7 (5), 511–518. https://doi.org/10.1130/L444.1.

Hudleston, P.J., 2015. Structures and fabrics in glacial ice: a review. J. Struct. Geol. 81, 1–27. https://doi.org/10.1016/j.jsg.2015.09.003.

Iaccarino, S., Montomoli, C., Carosi, R., Massonne, H., Visonà, D., 2017. Geology and tectono-metamorphic evolution of the Himalayan metamorphic core: insights from the Mugu Karnali transect, Western Nepal (Central Himalaya). J. Metamorph. Geol. 35, 301–325. https://doi.org/10.1111/jmg.12233.

Jones, D.B., Harrison, S., Anderson, K., Selley, H.L., Wood, J.L., Betts, R.A., 2018. The distribution and hydrological significance of rock glaciers in the Nepalese Himalaya. Glob. Planet. Chang. 160, 123–142. https://doi.org/10.1016/j.gloplacha.2017.11.005.

Jouanne, F., Mugnier, J.L., Sapkota, S.N., Bascou, P., Pecher, A., 2017. Estimation of coupling along the main Himalayan thrust in the central Himalaya. J. Asian Earth Sci. 133, 62–71. https://doi.org/10.1016/j.jseaes.2016.05.028.

Kääb, A., Berthier, E., Nuth, C., Gardelle, J., Arnaud, Y., 2012. Contrasting patterns of early twenty-first-century glacier mass change in the Himalayas. Nature 488 (7412), 495–498. https://doi.org/10.1038/nature11324.

Kayastha, R.B., Harrison, S.P., 2008. Changes of the equilibrium-line altitude since the little ice age in the Nepalese Himalaya. Ann. Glaciol. 48, 93–99. https://doi.org/10.3189/172756408784700581.

Kellett, D.A., Cottle, J.M., Larson, K.P., 2018. The South Tibetan Detachment System: history, advances, definition and future directions In Treloar, P.J., and Searle, M.P., (eds.) Himalayan Tectonics: A Modern Synthesis. Geological Society, London, Special Publications 483. https://doi.org/10.1144/SP483.2.

Lave, J., Avouac, J.P., 2001. Fluvial incision and tectonic uplift across the Himalayas of central Nepal. J. Geophys. Res. 106, 26561–26591. https://doi.org/10.1029/2001JB000359.

Montomoli, C., Iaccarino, S., Carosi, R., Langone, A., Visonà, D., 2013. Tectonometamorphic discontinuities within the Greater Himalayan Sequence in Western Nepal (Central Himalaya): insights on the exhumation of crystalline rocks. Tectonophysics, 608, 1349–1370. doi:https://doi.org/10.1016/j.tecto.2013.06.006.

Ohmura, A., Kasser, P., Funk, M., 1992. Climate at the equilibrium line of glaciers. J. Glaciol. 38 (130), 397–411. https://doi.org/10.1017/S0022143000002276.

Pedersen, V.K., Egholm, D.L., 2013. Glaciations in response to climate variations preconditioned by evolving topography. Nature 493 (7431), 206–210. https://doi.org/10.1038/nature11786.

Pedersen, V.K., Huismans, R.S., Herman, F., Egholm, D.L., 2014. Controls of initial topography on temporal and spatial patterns of glacial erosion. Geomorphology 223 (116), 96. https://doi.org/10.1016/j.geomorph.2014.06.028.

Pratt-Sitaula, B., Burbank, D.W., Heimsath, A.M., Humphrey, N.F., Oskin, M., Putkonen, J., 2011. Topographic control of asynchronous glacial advances: a case study from Annapurna, Nepal. Geophys. Res. Lett. 38 (24). https://doi.org/10.1029/2011GL049940.

Quade, J., Cater, J.M.L., Ojha, T.P., Adam, J., Harrison, T.M., 1995. Late Miocene environmental change in Nepal and the northern Indian subcontinent: stable isotopic evidence from paleosols. Geol. Soc. Am. Bull. 107, 1381–1397.

Quinn, J., 2001. Band Combinations. http://web.pdx.edu/~emch/ip1/bandcombinations.html.

Robinson, D.M., DeCelles, P.G., Copeland, P., 2006. Tectonic evolution of the Himalayan thrust belt in western Nepal: Implications for channel flow models. Bull. Geol. Soc. Am. 118 (7–8), 865–885. https://doi.org/10.1130/B25911.1.

Saylor, J., DeCelles, P.G., Gehrels, G.E., Murphy, M., Zhang, R., Kapp, P., 2010. Basin formation in the high Himalaya by arc-parallel extension and tectonic damming: Zhada Basin. Southwestern Tibet. Tectonics 29, 1. https://doi.org/10.1029/2008TC002390.

Scherler, D., Bookhagen, B., Strecker, M.R., 2011. Hillslope-glacier coupling: the interplay of topography and glacial dynamics in High Asia. Journal of Geophysical Research: Earth Surface 116 (2). https://doi.org/10.1029/2010JF001751.

Schoenbohm, L.M., Chen, J., Stutz, J., Sobel, E.R., Thiede, R.C., Kirby, B., Strecker, M.R., 2014. Glacial morphology in the Chinese Pamir: connections among climate, erosion, topography, lithology and exhumation. Geomorphology 221, 1–17. https://doi.org/10.1016/j.geomorph.2014.05.023.

Shugar, D.H., Clague, J.J., Best, J.L., Schoof, C., Willis, M.J., Copland, L., Roe, G.H., 2017. River piracy and drainage basin reorganization led by climate-driven glacier retreat. Nature Geoscience 10 (5), 370–375. https://doi.org/10.1038/ngeo2932.

Wagnon, P., Vincent, C., Arnaud, Y., Berthier, E., Vuillermoz, E., Gruber, S., Menegoz, M., Gilber, A., Dumont, M., Shea, J., Stumm, D., Pokhrel, B.K., 2013. Seasonal and annual mass balances of mera and pokalde glaciers (Nepal Himalaya) since 2007. Cryosphere 7 (6), 1769–1786. https://doi.org/10.5194/tc-7-1769-2013.

Ward, D.J., Anderson, R.S., Haeussler, P.J., 2012. Scaling the teflon peaks: rock type and the generation of extreme relief in the glaciated western Alaska range. Journal of Geophysical Research: Earth Surface 117 (1). https://doi.org/10.1029/2011JF002068.

Willett, S.D., McCoy, S.W., Taylor Perron, J., Goren, L., 2014. Dynamic reorganization of river basins. Science 343 (6175). https://doi.org/10.1126/science.1248765.